Cardinal Exponential Splines: Part II—Think Analog, Act Digital

Michael Unser, *Fellow, IEEE*

***Abstract*—By interpreting the Green-function reproduction property of exponential splines in signal processing terms, we uncover a fundamental relation that connects the impulse responses of allpole analog filters to their discrete counterparts. The link is that the latter are the B-spline coefficients of the former (which happen to be exponential splines). Motivated by this observation, we introduce an extended family of cardinal splines—the generalized E-splines—to generalize the concept for all convolution operators with rational transfer functions. We construct the corresponding compactly supported B-spline basis functions, which are characterized by their poles and zeros, thereby establishing an interesting connection with analog filter design techniques. We investigate the properties of these new B-splines and present the corresponding signal processing calculus, which allows us to perform continuous-time operations, such as convolution, differential operators, and modulation, by simple application of the discrete version of these operators in the B-spline domain. In particular, we show how the formalism can be used to obtain exact, discrete implementations of analog filters. Finally, we apply our results to the design of hybrid signal processing systems that rely on digital filtering to compensate for the nonideal characteristics of real-world analog-to-digital (A-to-D) and D-to-A conversion systems.**

***Index Terms*—Analog signal processing, A-to-D and D-to-A conversion, differential systems, filter design, hybrid signal processing, sampling, splines.**

I. Introduction

THE GAP between the continuous- and discrete-time—or analog versus digital—approaches to signal processing and electronic instrumentation, in general, has been widening ever since our technological society has entered the all-digital era. There is a strong tendency nowadays to emphasize and promote discrete signal processing techniques, as opposed to analog solutions. This is certainly justified by the current state of technology, as well as because there is a formal equivalence with continuous-time processing that is backed by Shannon's sampling theory. However, one should not forget that this equivalence, which holds for bandlimited functions only, excludes many practically relevant signals, in particular, those that are causal or of finite duration. The bandlimited hypothesis is an idealization, which is extremely useful for explaining basic concepts, but also has practical limitations; indeed, ideal lowpass filters are theoretical constructs that do not exist in the physical world, and real-world signals, at best, are only essentially bandlimited [1]. Interestingly enough, and despite the fact that the technological move to digital is almost complete, there has been a recent revival of continuous-time signal processing thinking that has been triggered, for the most part, by recent advances in wavelet theory [2]–[4]. The powerful notions of multiresolution analysis [5], self-similarity (e.g., fractals) [6], singularity analysis [7], and even the more mundane task of signal interpolation [8], [9], are undissociable from a continuous-time interpretation. It is therefore crucial to have efficient mathematical tools at our disposal that allow us to easily switch from one domain to the other—and this is precisely the niche that splines, and to some extent wavelets, are trying to fill.

Our purpose in this paper is to present a unifying continuous/discrete approach to signal processing that departs from the traditional bandlimited formulation. Our motivation and general philosophy is summarized by the motto "think analog, act digital." Indeed, we believe that there are many signal processing problems that are better suited for a continuous-time domain formulation, even though one is ultimately looking for solutions that should be transposable into efficient digital signal processing algorithms. Typical examples are the implementation of fractional delays [10], [11], the evaluation of differential operators [12]–[15], signal interpolation, and approximation for sampling-rate conversion [16], [17], as well as the whole class of wavelet-based signal analysis techniques. Another important category that should benefit from a unifying formulation is hybrid signal processing, which combines analog and discrete components.

The starting point for the present formulation is the signal processing theory of exponential splines that was developed in a companion paper [18]. In Section II, we apply these results to uncover a remarkable link between the elementary analog signals of classical system theory (causal exponentials/polynomials) and their discrete-time counterparts. Unlike the classical bandlimited approach, the present formulation uses compactly supported basis functions and allows for an exact representation of the continuous-time response of an allpole system. In Section III, we extend the class of cardinal exponential splines to encompass the reponse of operators with rational transfer functions. Specifically, we show that the poles and zeros of an analog filter uniquely specify a subspace of generalized E-splines which admits a B-spline-like Riesz basis. We also present an extended calculus for the exact computation of continuous-time signal processing operators. In Section IV, we apply these techniques to the discrete implementation of analog filters. The approach that we propose constitutes an

Manuscript received November 26, 2003; revised April 16, 2004. This work was supported in part by Grant 200020-101821 from the Swiss National Science Foundation. The associate editor coordinating the review of this manuscript and approving it for publication was Prof. Karim Drouiche.

The author is with the Biomedical Imaging Group, EPFL, CH-1015 Lausanne, Switzerland (e-Mail: michael.unser@epfl.ch).

Digital Object Identifier 10.1109/TSP.2005.843699

1053-587X/$20.00 © 2005 IEEE

TABLE I
BASIC CONTINUOUS-TIME CONVOLUTION OPERATORS

Operator	Notation	Impulse response	Frequency response
Identity	$\mathrm{I}\{\ \}$	$\delta(t)$	1
Shift	$S_\tau\{f\} = f(t-\tau)$	$\delta(t-\tau)$	$e^{-j\omega\tau}$
Integral	$\mathrm{D}^{-1}\{\ \} = \int_{-\infty}^{t} dt$	$1_+(t)$	$\pi\delta(\omega) + \frac{1}{j\omega}$
Multiple integral	$\mathrm{D}^{-n}\{\ \}$	$\frac{t_+^{n-1}}{(n-1)!}$	$\frac{j^{n-1}\pi\delta^{(n-1)}(\omega)}{(n-1)!} + \frac{1}{(j\omega)^n}$
Simple differential system	$(\mathrm{D}-\alpha\mathrm{I})^{-1}\{\ \}$	$1_+(t)\cdot e^{\alpha t}$	$\frac{1}{j\omega-\alpha}$ $\mathrm{Re}\{\alpha\}<0$
Iterated differential system	$(\mathrm{D}-\alpha\mathrm{I})^{-n}\{\ \}$	$\frac{t_+^{n-1}e^{\alpha t}}{(n-1)!}$	$\frac{1}{(j\omega-\alpha)^n}$ $\mathrm{Re}\{\alpha\}<0$

TABLE II
ELEMENTARY CAUSAL DISCRETE-TIME SIGNALS

Name	Discrete time specification	z-transform
Unit impulse	$\delta[k]$	1
Shift	$\delta[k-k_0]$	z^{-k_0}
Unit step	$p_0[k] = \begin{cases} 0, & k<0 \\ 1, & k\geq 0 \end{cases}$	$\frac{1}{1-z^{-1}}$
Discrete mononial	$p_0^{[n-1]}[k] = \begin{cases} 0, & k<0 \\ \prod_{m=1}^{n-1}(k+m), & k\geq 0 \end{cases}$	$\frac{1}{(1-z^{-1})^n}$
Causal exponential	$p_\alpha[k] = \begin{cases} 0, & k<0 \\ e^{\alpha k}, & k\geq 0 \end{cases}$	$\frac{1}{1-e^{\alpha}z^{-1}}$
Discrete exponential monomial	$p_\alpha^{[n-1]}[k] = \begin{cases} 0, & k<0 \\ e^{\alpha k}\prod_{m=1}^{n-1}(k+m), & k\geq 0 \end{cases}$	$\frac{1}{(1-e^{\alpha}z^{-1})^n}$

interesting alternative to more traditional analog-to-discrete conversion techniques such as the impulse invariance method (also included in our formulation) and the bilinear transform. Finally, in Section V, we apply our formalism to the design of hybrid signal processing systems that use digital techniques to compensate for the distortions inflicted by nonideal analog-to-digital (A-to-D) and D-to-A conversion.

II. BRIDGING THE GAP BETWEEN THE DISCRETE AND THE CONTINUOUS

In this section, we reinterpret some of the basic results in [18] and show that the exponential B-splines have an important conceptual role in that they connect some fundamental aspects of discrete and continuous-time signal processing.

A. B-Splines as Discrete-to-Continuous Translators

The basic continuous-time convolution operators that are encountered in most courses on signals and systems are listed in Table I [19], [20]. These are characterized either by their impulse response $h(t)$ or their frequency response $\hat{h}(\omega) = \mathcal{F}\{h(t)\}$, which is defined as $\hat{h}(\omega) = \int_{-\infty}^{+\infty} h(t)e^{-j\omega t}\mathrm{d}t$ when $h(t) \in L_1$. The discrete-time counterpart of these operators are given in Table II, together with their z-transform. The Fourier transform of these sequences are obtained by making the substitution $z = e^{j\omega}$. Note that the two upper rows in Tables I and II describe distortion-free systems (identity or pure delay), while the four bottom rows correspond to allpole systems. The link between the two

TABLE III
D-TO-A TRANSLATING B-SPLINES: THE INTEGER SHIFTS OF THESE B-SPLINES ARE THE BASIS FUNCTIONS THAT ALLOW THE RECONSTRUCTION OF THE IMPULSE RESPONSES IN TABLE I FROM THE DISCRETE SIGNALS IN TABLE II

B-spline	Operator L	Order N	Frequency response
$\delta(t)$	$I\{\ \}$	0	1
$\delta(t-\tau)$	$S_\tau\{\ \}$	0	$e^{-j\omega\tau}$
$\beta_{(0)}(t)$	$D\{\ \} = \frac{d}{dt}$	1	$\frac{1-e^{-j\omega}}{j\omega}$
$\beta_{(0,\cdots,0)}(t)$	$D^n\{\ \}$	n	$\left(\frac{1-e^{-j\omega}}{j\omega}\right)^n$
$\beta_\alpha(t)$	$(D-\alpha I)\{\ \}$	1	$\frac{1-e^{\alpha-j\omega}}{j\omega-\alpha}$
$\beta_{(\alpha,\cdots,\alpha)}(t)$	$(D-\alpha I)^n\{\ \}$	n	$\left(\frac{1-e^{\alpha-j\omega}}{j\omega-\alpha}\right)^n$

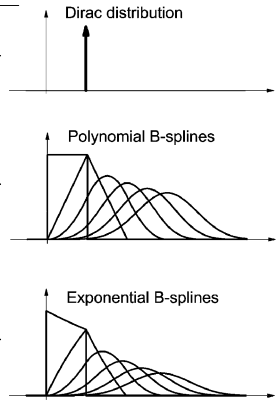

tables is that, for each row, the poles are in exact correspondence through the mapping $z = e^s$, or $s = \log z$, that connects the Laplace and the z-transform (cf. [20, p. 695]). We also note that there is a family resemblance between the analog and discrete signals in corresponding rows, even though the connection is not necessarily as simple as the sampling relation that holds for the first-order systems (unit step and simple exponential).

In fact, the mathematical relation between these two tables is provided by the Green-function reproduction formula

$$\rho_{\vec{\alpha}}(t) = \sum_{k=0}^{+\infty} p_{\vec{\alpha}}[k]\ \beta_{\vec{\alpha}}(t-k) \tag{1}$$

that we have encountered in Part I of this paper [18]. The corresponding B-spline functions are represented in Table III. In the present situation, the Green function $\rho_{\vec{\alpha}}(t) = \mathrm{L}_{\vec{\alpha}}^{-1}\{\delta(t)\} = \mathrm{H}_{\vec{\alpha}}\{\delta(t)\}$ is the impulse response $h(t)$ of the system $\mathrm{H}_{\vec{\alpha}}$, which is the causal inverse of the exponential-spline defining operator $\mathrm{L}_{\vec{\alpha}}$. This simply means that the discrete signals in Table II are the B-spline coefficients of the impulse responses in Table I. The case of the Dirac distribution is also covered by our formulation, provided that we define $\delta(t)$ (or, $\delta(t-\tau_0)$) as a B-spline of order zero.

Another perhaps even more illuminating way to understand the connection is to observe that the Fourier transforms of the B-splines in Table III are obtained by dividing the analog ones in Table I by the discrete ones in Table II. The remarkable consequence of forming this ratio is that the poles of the analog system are cancelled by the $j2\pi$-periodic zeros of the B-spline numerator, which are precisely the poles of the discrete system in Table II. Another beneficial side effect of this division is the zeroing of the Dirac distributions appearing in the third and fourth row of Table I.

To exemplify this link, we give the explicit time-domain formulae that relate—and also specify—the signals in the bottom row of Tables I–III:

$$t_+^{n-1}e^{\alpha t} = \sum_{k=0}^{+\infty} \binom{n-1+k}{k} \beta_{(\alpha,\ldots,\alpha)}(t-k) \tag{2}$$

where the relevant B-spline of order and multiplicity n is given by

$$\beta_{(\alpha,\ldots,\alpha)}(t)=\sum_{k=0}^{n}\binom{n}{k}(-e^{\alpha})^{k}(t-k)_{+}^{n-1}e^{\alpha(t-k)}$$
$$=e^{\alpha t}\sum_{k=0}^{n}\binom{n}{k}(-1)^{k}(t-k)_{+}^{n-1}=e^{\alpha t}\cdot\beta_{(0,\ldots,0)}(t). \tag{3}$$

This latter formula is obtained by inverse Fourier transformation of the expression in the bottom row in Table III. The crucial step for this computation is to expand $(1-e^{\alpha}e^{-j\omega})^{n}$ using the binomial formula and to interpret each factor $e^{-j\omega k}$ as a shift operator. Note that (2) and (3) extend two well-known relations for polynomial splines that correspond to the case $\alpha=0$.

B. Differential Interpretation of the Localization Operator

The spline-defining differential operator $\mathrm{L}_{\vec{\alpha}}=\mathrm{D}^{N}+a_{N-1}\mathrm{D}^{N-1}+\cdots+a_{0}\mathrm{I}$ is entirely characterized by the zeros α_n, $n=1,\ldots,N$ of its characteristic polynomial $L_{\vec{\alpha}}(s)=\prod_{n=1}^{N}(s-\alpha_n)$. These zeros also specify its null space $\mathcal{N}_{\vec{\alpha}}$. The time-domain equivalent of the frequency-domain division process that has been described is the B-spline generating formula $\beta_{\vec{\alpha}}(t)=\Delta_{\vec{\alpha}}\{\rho_{\vec{\alpha}}(t)\}$, where $\Delta_{\vec{\alpha}}$ is the localization operator and $\rho_{\vec{\alpha}}(t)$ the Green function of $\mathrm{L}_{\vec{\alpha}}$. This is consistent with the property that the Fourier transform of $\Delta_{\vec{\alpha}}\{\delta(t)\}=\sum_{k=0}^{N}d_{\vec{\alpha}}[k]\delta(t-k)$, which is given by

$$\Delta_{\vec{\alpha}}(e^{j\omega})=\prod_{n=1}^{N}(1-e^{\alpha_n-j\omega})=\frac{1}{P_{\vec{\alpha}}(e^{j\omega})} \tag{4}$$

is the inverse of that of $p_{\vec{\alpha}}[k]$ in (1). The Laplace transform $\Delta_{\vec{\alpha}}(s)$ is obtained by making the formal substitution $j\omega=s$ in (4); this function vanishes for $s=\alpha_n+j2\pi k$, $k\in\mathbb{Z}$, $n=1,\ldots,N$, meaning that it has zeros in perfect correspondence with those of $L_{\vec{\alpha}}(s)$. Consequently, $\Delta_{\vec{\alpha}}$ has the same ability as $\mathrm{L}_{\vec{\alpha}}$ to annihilate the exponential polynomials in $\mathcal{N}_{\vec{\alpha}}$. We may therefore think of $\Delta_{\vec{\alpha}}$, which is equivalent to a digital FIR filtering with $d_{\vec{\alpha}}[k]$, as a discrete approximation of $\mathrm{L}_{\vec{\alpha}}$. This interpretation is further justified by the remarkable distributional identity

$$\forall f\in S',\ \ \Delta_{\vec{\alpha}}\{f\}=\beta_{\vec{\alpha}}*\mathrm{L}_{\vec{\alpha}}\{f\}$$

which is a direct consequence of the Fourier definition of the B-spline. Here, S' stands for Schwartz's class of tempered distributions. This shows that the discrete operator $\Delta_{\vec{\alpha}}$ provides a smoothed version (convolution with the corresponding B-spline) of the continuous one. It also guarantees that the distortion effect is maximally localized because of the minimum-support property of the B-spline. Likewise, we have the scaled version of this equation

$$\forall f\in S',\ \ \Delta_{\vec{\alpha},T}\{f\}=\frac{1}{T}\beta_{\vec{\alpha},T}*\mathrm{L}_{\vec{\alpha}}\{f\}$$

which characterizes the convergence of the discrete operator to the continuous one as the sampling step goes to zero. In the limit, we have a perfect identity due to the property that $(1/T)\beta_{\vec{\alpha},T}(t)$ converges to $\delta(t)$ as $T\to 0$.

III. Generalized Exponential Splines

The discrete-to-continuous connection that has been described in Section II-A is appealing; unfortunately, in its current version, it is only applicable to allpole systems. This motivates us to extend the exponential spline family and the corresponding signal processing framework by considering a more general class of differential operators.

A. Extending the Family to Rational Operators

The exponential splines that we have investigated in [18] are associated with ordinary differential operators whose transfer functions are polynomials. To extend the family, we propose to consider the richer class of operators with rational transfer functions. To this end, we introduce the augmented parameter vector $\vec{\alpha}=(\alpha_1,\ldots,\alpha_N;\ \gamma_1,\ldots,\gamma_M)$ with $M<N$, which specifies the new spline-defining operator $\mathrm{L}_{\vec{\alpha}}\{\cdot\}$, whose transfer function is given by

$$L_{\vec{\alpha}}(s)=\frac{\prod_{n=1}^{N}(s-\alpha_n)}{\prod_{m=1}^{M}(s-\gamma_m)} \tag{5}$$

with $\gamma_m\neq\alpha_n$ for all m and n. The null space of this operator, which is denoted by $\mathcal{N}_{\vec{\alpha}}$, is determined by the zeros of $L_{\vec{\alpha}}(s)$, which do not depend on the denominator. Consequently, $\mathcal{N}_{\vec{\alpha}}$, which is of dimension N, remains the same as before.

We can then define a generalized exponential spline in exactly the same terms as before (cf. [18, Def. 1]): $s(t)$ is a generalized E-spline with parameter $\vec{\alpha}$ if and only if $\mathrm{L}_{\vec{\alpha}}\{s(t)\}$ is a weighted sum of Dirac impulses that are positioned at the knots (spline singularities). Note that we are not imposing any restriction on $\mathrm{L}_{\vec{\alpha}}$: The γ_m's can be freely chosen and need not be located in the left complex plane.

To construct the corresponding splines, we must specify the Green function of $\mathrm{L}_{\vec{\alpha}}$, which is equivalent to determining the impulse response of the causal inverse operator $\mathrm{H}_{\vec{\alpha}}$, whose Laplace transform is

$$H_{\vec{\alpha}}(s)=\frac{\prod_{m=1}^{M}(s-\gamma_m)}{\prod_{n=1}^{N}(s-\alpha_n)}. \tag{6}$$

This leads to the following generic representation of a generalized E-spline with parameter $\vec{\alpha}$ and knots $-\infty<\cdots t_k<t_{k+1}<\cdots<+\infty$

$$s(t)=\sum_{k}a_k\rho_{\vec{\alpha}}(t-t_k)+p_0(t) \tag{7}$$

with $\rho_{\vec{\alpha}}(t)=\mathcal{L}^{-1}\{H_{\vec{\alpha}}(s)\}$, where $\mathcal{L}^{-1}$ stands for the inverse Laplace transform; $p_0(t)\in\mathcal{N}_{\vec{\alpha}}$ is a global exponential polynomial component that is selected such as to satisfy some additional boundary conditions (N linear constraints). The Green function takes essentially the same form as before:

$$\rho_{\vec{\alpha}}(t)=\sum_{m=1}^{N_d}\sum_{n=1}^{n_{(m)}}c_{m,n}\frac{t_{+}^{n-1}}{(n-1)!}e^{\alpha_{(m)}t} \tag{8}$$

where the $c_{m,n}$'s are the coefficients of the partial fraction decomposition of $H_{\vec{\alpha}}(s)$ in (6). The important difference, which is is due to the presence of the numerator in (6), is that $\rho_{\vec{\alpha}}(t)\in C^{N-M-2}$ (the class of functions with continuous derivatives up

to order $N-M-2$), meaning that it has a lesser degree of differentiability than before. While these splines still coincide with a function in $\mathcal{N}_{\vec{\alpha}}$ within each interval $[t_k, t_{k+1})$, their nature has become somewhat different because the pieces are no longer connected together as smoothly as before. Technically, they are no longer *T*-splines nor even *L*-splines, according to the general definition of these splines given in [21].

B. Generalized Exponential B-Splines

From now on, we focus again on the cardinal splines that have their knots at the integers. The first important step is to construct some local (i.e., compactly supported and shortest-possible) basis functions for these spline spaces, which can be done in essentially the same fashion as in the standard case. This leads us to the definition of the generalized B-spline of order N with parameter $\vec{\alpha} = (\alpha_1, \ldots, \alpha_N;\ \gamma_1, \ldots, \gamma_M)$:

$$\beta_{\vec{\alpha}}(t) = \Delta_{\vec{\alpha}}\{\rho_{\vec{\alpha}}(t)\} \tag{9}$$

where $\rho_{\vec{\alpha}}(t) = \mathcal{L}^{-1}\{1/L_{\vec{\alpha}}(s)\}$ with $L_{\vec{\alpha}}(s)$ specified by (5), and where the localization operator is the same before, i.e., $\Delta_{\vec{\alpha}}\{f(t)\} = \sum_{k=0}^{N} d_{\vec{\alpha}}[k] f(t-k)$, where the Fourier transform of $d_{\vec{\alpha}}[k]$ is given by (4).

It is easy to see that these generalized Nth-order B-splines are supported in $[0, N)$. The argument is that they can be generated from the standard ones by applying the differential operator $\mathrm{L}_{\vec{\gamma}} = (\mathrm{D} - \gamma_M \mathrm{I}) * \cdots * (\mathrm{D} - \gamma_1 \mathrm{I})$, whose impulse response is a point distribution. This also explains why their regularity is reduced by M, i.e, $\beta_{\vec{\alpha}}(t) \in C^{N-M-2}$.

Note that the generalized exponential B-spline $\beta_{\vec{\alpha}}(t)$ is well-defined (bounded and compactly supported) as long as $M < N$, irrespective of the stability of $\mathrm{H}_{\vec{\alpha}} = \mathrm{L}_{\vec{\alpha}}^{-1}$. Its Fourier transform is given by

$$\hat{\beta}_{\vec{\alpha}}(\omega) = \left(\prod_{n=1}^{N} \frac{1 - e^{\alpha_n - j\omega}}{j\omega - \alpha_n} \right) \cdot \prod_{m=1}^{M} (j\omega - \gamma_m). \tag{10}$$

We will therefore refer to the α_n's as the poles of the B-spline and to the γ_m's as the (nonperiodic) zeros.

The class of these new B-splines is obviously much richer that the standard E-splines, not to mention the polynomial ones. Interestingly, the family contains some known basis functions that have not been classified as splines so far. A notable example is the family of maximum order, minimum support (MOMS) functions that has been characterized in [22]. They correspond to the parametrization $\alpha_n = 0$, $n = 1, \ldots, N$ and $\gamma_m \in \mathbb{R}$, $m = 1, \ldots, M$. Three prominent fourth-order members of the MOMS family are shown in Fig. 1: the cubic B-spline with $\vec{\alpha} = (0,0,0,0)$, the O-MOM with $\vec{\alpha} = (0,0,0,0; -j\sqrt{42}, j\sqrt{42})$, and the cubic Lagrange interpolator with $\vec{\alpha} = (0,0,0,0; \sqrt{6}, -\sqrt{6})$.

C. B-Spline Properties

The generalized B-splines have essentially the same properties as the standard ones (cf. [18, Sec. II.B]). The only critical difference is that one has to adapt the B-spline composition rule, keeping the poles and zeros separate. This means that the concatenation of the augmented parameter vectors $\vec{\alpha}_1$ and $\vec{\alpha}_2$ of size $N_1 + M_1$ and $N_2 + M_2$, respectively, now yields the vector

$$(\vec{\alpha}_1 : \vec{\alpha}_2) = (\alpha_{1,1}, \ldots, \alpha_{1,N_1}, \alpha_{2,1}, \ldots, \alpha_{2,N_2};\ \gamma_{1,1}, \ldots, \gamma_{1,M_1}, \gamma_{2,1}, \ldots, \gamma_{2,M_2})$$

which is of size $(N_1+N_2)+(M_1+M_2)$. With this convention, we can write the generalized B-spline convolution formula

$$\left(\beta_{\vec{\alpha}_1} * \beta_{\vec{\alpha}_2}\right)(t) = \beta_{(\vec{\alpha}_1 : \vec{\alpha}_2)}(t) \tag{11}$$

which is easily established in the Fourier domain.

As in the standard case, changing the sign of the roots (poles and zeros) has a mirroring effect

$$\beta_{-\vec{\alpha}}(t) = (-1)^M \left(\prod_{n=1}^{N} e^{-\alpha_n} \right) \beta_{\vec{\alpha}}(-t + N) \tag{12}$$

Thus, in order to construct symmetric basis functions, we have to select roots that are either zero or grouped in pairs of poles (or zeros) of opposite sign. Symmetry is a property that is desirable for image processing applications.

The formula for the cross-correlation of two generalized B-splines also needs to be adapted slightly:

$$\begin{aligned} \langle \beta_{\vec{\alpha}_1}(\cdot), \beta_{\vec{\alpha}_2}(\cdot + \tau) \rangle &= \left(\beta_{\vec{\alpha}_1} * \beta^H_{\vec{\alpha}_2}\right)(\tau) \\ &= (-1)^{M_1} \left(\prod_{n=1}^{N_1} e^{\alpha_{1,n}} \right) \beta_{(-\vec{\alpha}_1 : \vec{\alpha}_2^*)}(\tau + N_1) \end{aligned} \tag{13}$$

with the notation $f^H(t) := f^*(-t)$.

D. B-Splines Representation

The B-spline representation theorem in [18] can also be extended for the generalized E-splines.

Theorem 1: The set of functions $\{\beta_{\vec{\alpha}}(t-k)\}_{k \in \mathbb{Z}}$ provides a Riesz basis of $V_{\vec{\alpha}}$—the space of cardinal generalized E-splines with finite energy—if and only if $\alpha_n - \alpha_m \neq j2\pi k$, $k \in \mathbb{Z}$ for all pairs of distinct, purely imaginary poles.

This is established by adapting the proof of [18], which carries over without difficulty if we make use of the following properties.

1) The null space is the same as in the standard case, as we have already mentioned.
2) The Green-function reproduction formula (1) is still valid, provided that one uses the appropriate general-

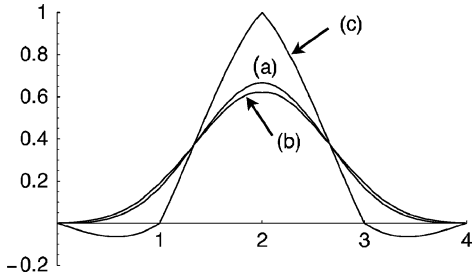

Fig. 1. Three generalized B-splines of order $N = 4$. (a) Cubic B-spline. (b) Cubic OMOMS. (c) Cubic Lagrange interpolator. To facilitate the comparison, the B-splines have been normalized to have a unit integral.

ized B-spline. This is because the localization operator is the same as in the standard case.

3) The exponential polynomial reproduction property is still true as well. Indeed, we have already mentioned that the generalized B-splines include a standard B-spline convolution factor, which makes them inherit the polynomial reproduction property (by [18, Prop. 1]). The necessary condition is $L_{\vec{\gamma}}(s) \neq 0$ for $s = \alpha_n$, which is obviously satisfied as long as $\alpha_n \neq \gamma_m$, $\forall m, n$.

4) The Riesz-basis condition is satisfied. The upper bound is well-defined because the Gram sequence $a_{\vec{\alpha}}$ is in ℓ_1. The lower bound exists as well because the additional factors $(j\omega - \gamma_m)$ in (10) cannot induce any 2π-periodic vanishing of $\hat{\beta}_{\vec{\alpha}}(\omega)$.

The Riesz bounds can be computed as described in [18, Eqs. (30) and (31)], provided that one uses the following extended formula for the calculation of the Gram sequence:

$$a_{\vec{\alpha}}[k] = \langle \beta_{\vec{\alpha}}(\cdot), \beta_{\vec{\alpha}}(\cdot - k) \rangle = (-1)^M \left(\prod_{n=1}^{N} e^{\alpha_n^*} \right) \beta_{(\vec{\alpha}:-\vec{\alpha}^*)}(N + k). \quad (14)$$

To facilitate this type of computations, we have written Mathematica software that symbolically evaluates the generalized B-splines and other related quantities for any given parameter vector $\vec{\alpha}$. This package is briefly described in the Appendix and is made available to the research community over the World Wide Web.

E. Continuous-Discrete Signal Processing

Many of the formulae in Part I, Section III, remain valid for our generalized splines, the reason being that the effect of the new zeros is entirely absorbed in the B-spline basis functions. However, there are also a few additions to the spline calculus because the class of functions has become richer.

1) Interpolation: The interpolation procedure is the same as in the standard case. However, we now have considerably more freedom for designing new basis functions, which could be advantageous for applications such as high-quality image interpolation [8]. In particular, we note that the best interpolation methods known to date are either based on polynomial splines or on OMOMS [22], which are both part of our enlarged family. This opens up the quest for even better ones.

2) Convolution: The convolution procedure carries over directly because of the generalized B-spline convolution property (11).

3) Modulation: The modulation property is unchanged, except that its generalized version also requires the frequency shifting of the zeros. Interestingly, our exponential spline family is closed under an even more general operation, which is the modulation with a complex exponential $e^{s_0 t}$ for arbitrary $s_0 \in \mathbb{C}$.

Proposition 1: Let $s(t) = \sum_{k \in \mathbb{Z}} c_k \, \beta_{\vec{\alpha}}(t - k)$ be a spline signal with exponential parameter $\vec{\alpha} = (\alpha_1, \ldots, \alpha_N; \gamma_1, \ldots, \gamma_M)$. Then, the exponentially modulated signal $e^{s_0 t} \cdot s(t)$, with $s_0 \in \mathbb{C}$, is a spline with exponential parameter $\vec{\alpha} + \vec{1} s_0 = (\alpha_1 + s_0, \ldots, \alpha_N + s_0; \ \gamma_1 + s_0, \ldots, \gamma_M + s_0)$ that is given by

$$s(t) \cdot e^{s_0 t} = \sum_{k \in \mathbb{Z}} c_k \, e^{s_0 k} \, \beta_{\vec{\alpha} + \vec{1} s_0}(t - k). \quad (15)$$

Proof: We compute the Laplace transform of the exponentially modulated B-spline

$$\mathcal{L}\{e^{s_0 t} \cdot \beta_{\vec{\alpha}}(t)\} = \int_0^{+\infty} \beta_{\vec{\alpha}}(t) e^{-(s - s_0)t} \, \mathrm{d}t = \prod_{m=1}^{M} (s - s_0 - \gamma_m) \left(\prod_{n=1}^{N} \frac{1 - e^{\alpha_n - (s - s_0)}}{s - s_0 - \alpha_n} \right)$$

which also yields the Fourier transform if we replace s by $j\omega$. This clearly shows that $e^{s_0 t} \cdot \beta_{\vec{\alpha}}(t) = \beta_{\vec{\alpha} + \vec{1} s_0}(t)$, where $\vec{1} = (1, \ldots, 1)$. Next, we note that $e^{s_0 t} \cdot \beta_{\vec{\alpha}}(t - k) = e^{s_0 k} \cdot \beta_{\vec{\alpha} + \vec{1} s_0}(t - k)$, which we then substitute in the B-spline representation of the modulated signal. ∎

Note that this property can be used to derive the relation (3) that connects the exponential B-spline of multiplicity N to its polynomial B-spline counterpart.

4) Differential Operators: The differential formula given by [18, Eq. (37)] is still valid when $\vec{\alpha}_1$ consists of poles only. However, the family of B-splines is now rich enough so that we can generalize the procedure for arbitrary differential operators.

Proposition 2: Let $\mathrm{L}_{\vec{\gamma}'}\{\cdot\}$ be the differential operator of order M', whose Laplace transform is $L_{\vec{\gamma}'}(s) = \prod_{m=1}^{M'} (s - \gamma'_m)$. Then, we have the explicit B-spline differential relations

$$\mathrm{L}_{\vec{\gamma}'}\{\beta_{\vec{\alpha}}(t)\} = \beta_{(\alpha_1, \ldots, \alpha_N; \, \gamma_1, \ldots, \gamma_M, \gamma'_1, \ldots, \gamma'_{M'})}(t) \quad (16)$$

$$\mathrm{L}_{\vec{\gamma}'}\{\beta_{(\vec{\gamma}':\vec{\alpha})}(t)\} = \Delta_{\vec{\gamma}'}\{\beta_{\vec{\alpha}}\}(t) \quad (17)$$

where the conditions for the validity of (16) are $\gamma'_m \neq \alpha_n$, $\forall m, n$, and $M' + M \leq N$; there is no restriction for (17).

Proof: These relations are easily derived in the Fourier domain. The second one, for instance, is obtained through the following manipulation [cancellation of the factors $(j\omega - \gamma'_m)$]

$$\mathcal{F}\{\mathrm{L}_{\vec{\gamma}'}\{\beta_{(\vec{\gamma}':\vec{\alpha})}(t)\} = \prod_{m=1}^{M'} (j\omega - \gamma'_m) \cdot \hat{\beta}_{(\vec{\gamma}':\vec{\alpha})}(\omega) = \prod_{m=1}^{M'} (1 - e^{\gamma'_m - j\omega}) \underbrace{\frac{\prod_{n=1}^{N} (1 - e^{\alpha_n - j\omega}) \prod_{m=1}^{M} (j\omega - \gamma_m)}{\prod_{n=1}^{N} (j\omega - \alpha_n)}}_{\hat{\beta}_{\vec{\alpha}}(\omega)}.$$

∎

5) Dilation by m: Here, there is a slight change that requires an extended definition of the generalized spline scaling filter

$$H_{\vec{\alpha},m}(z) = \frac{1}{m^{N-1-M}} \prod_{n=1}^{N} \frac{1 - e^{m\alpha_n} z^{-m}}{1 - e^{\alpha_n} z^{-1}} \quad (18)$$

which has a mild dependence on the zeros through their number M, meaning that the same filter is shared by different types of splines. As in the standard case, the filter is FIR of size $mN - 1$,

which is not immediately apparent from its rational representation.

Proposition 3: The generalized exponential B-spline with parameter $\vec{\alpha}$ satisfies the m-dilation relation

$$\beta_{\vec{\alpha}}\left(\frac{t}{m}\right) = \sum_{k\in\mathbb{Z}} h_{\vec{\alpha}/m,m}[k]\beta_{\vec{\alpha}/m}(t-k) \tag{19}$$

where $h_{\vec{\alpha}/m,m}[k]$ is the impulse response of the filter (18) with rescaled exponential parameter $(\alpha_1/m,\ldots,\alpha_N/m;\ \gamma_1/m,\ldots,\gamma_M/m)$.

Proof: The result is established by direct manipulation in the Fourier domain:

$$\begin{aligned}
&\mathcal{F}\left\{\beta_{\vec{\alpha}}\left(\frac{t}{m}\right)\right\}\\
&= m\cdot\hat{\beta}_{\vec{\alpha}}(m\omega)\\
&= m\prod_{n=1}^{N}\frac{1-e^{\alpha_n-jm\omega}}{jm\omega-\alpha_n}\prod_{m'=1}^{M}(jm\omega-\gamma'_m)\\
&= \frac{m^{M+1}}{m^N}\prod_{n=1}^{N}\frac{1-e^{\alpha_n}e^{-jm\omega}}{1-e^{\alpha_n/m}e^{-j\omega}}\underbrace{\prod_{n=1}^{N}\frac{1-e^{\alpha_n/m-j\omega}}{j\omega-\frac{\alpha_n}{m}}\prod_{m'=1}^{M}\left(j\omega-\frac{\gamma'_m}{m}\right)}_{\hat{\beta}_{\vec{\alpha}/m}(\omega)}
\end{aligned} \tag{20}$$

where the two factors on the right-hand side can be readily identified. Note that the division/multiplication by $(1-e^{\alpha_n/m}e^{-j\omega})$ is legitimate even when there are roots on the unit circle since the zeros of the denominator are cancelled by those of the numerator—this is precisely the reason why the filter $H_{\vec{\alpha},m}(z)$ in (18) and the exponential B-spline are both FIR! ■

IV. Discrete Implementation of Analog Filters

Shannon's sampling theory guarantees that there is a perfect equivalence between continuous- and discrete-time signal processing techniques for bandlimited functions. Unfortunately, the bandlimited hypothesis excludes all physically realistic signals. In particular, it is incompatible with causality,[1] meaning that it is impossible to exactly represent the impulse response of analog filters, including all the elementary signals in Table I, within the classical bandlimited framework. We will now show how the present formalism can circumvent this limitation and yield exact computational schemes for implementing continuously defined signal processing operators in the discrete B-spline domain.

A. Analog Filtering in the B-Spline Domain

We consider the task of evaluating $y(t) = \mathrm{H}_{\vec{\alpha}}\{x(t)\}$, where $x(t)$ is some continuously defined input signal and where $\mathrm{H}_{\vec{\alpha}}$ is a stable analog filter whose rational transfer function is given by (6). Because of the stability hypothesis, the poles of $H_{\vec{\alpha}}(s)$ are in the open left complex plane (i.e., $\mathrm{Re}(\alpha_n) < 0, \forall n$), which ensures that the impulse response of the system $\rho_{\vec{\alpha}}(t) = \mathrm{H}_{\vec{\alpha}}\{\delta(t)\}$ is in $L_2 \cap L_1$.

[1]In fact, it is much worse than that: One cannot construct a nonzero bandlimited signal $f(t)$ such that $f(t) = 0, \forall t \in [t_1, t_2]$ for any $t_1 < t_2$.

We assume that the input signal is an exponential spline with parameter $\vec{\alpha}_1$ specified by its B-spline expansion:

$$x(t) = \sum_{k\in\mathbb{Z}} c_1[k]\beta_{\vec{\alpha}_1}(t-k).$$

This representation is either given to us or is fitted to a series of input samples $\{x[k]\}_{k\in\mathbb{Z}}$ using the interpolation procedure discussed in [18, Sec. III.B]. Note that this model also covers the case of idealized sampling since $\delta(t)$ is formally equivalent to a B-spline of order 0.

From the theory in Section III, we know that $\rho_{\vec{\alpha}}(t)$ is a generalized E-spline with parameter $\vec{\alpha}$ and that its B-spline representation is given by (1) (Green-function reproduction formula). Since the poles are in the left complex plane, the allpole digital filter $P_{\vec{\alpha}}(z) = \Delta_{\vec{\alpha}}^{-1}(z) = \prod_{n=1}^{N}(1-e^{\alpha_n}z^{-1})^{-1}$ is stable as well, implying that the B-spline coefficients $p_{\vec{\alpha}}[k]$ in (1) are decaying exponentially fast.

The output signal $y(t) = (\rho_{\vec{\alpha}} * x)(t)$ can now be easily calculated thanks to the B-spline convolution property

$$y(t) = \int_{-\infty}^{+\infty}\sum_{k_1\in\mathbb{Z}} c_1(k_1)\beta_{\vec{\alpha}_1}(\tau-k_1)\sum_{k\in\mathbb{Z}} p_{\vec{\alpha}}[k]\beta_{\vec{\alpha}}(t-\tau-k)\,\mathrm{d}\tau \tag{21}$$

$$= \sum_{k\in\mathbb{Z}}\underbrace{(c_1 * p_{\vec{\alpha}})[k]}_{c_2[k]}\beta_{(\vec{\alpha}_1:\vec{\alpha})}(t-k). \tag{22}$$

This shows that $y(t)$ is an E-spline with parameter $\vec{\alpha}_2 = (\vec{\alpha}_1 : \vec{\alpha})$ and that its B-spline coefficients $c_2[k]$ are obtained by applying the digital filter $P_{\vec{\alpha}}(z)$ to the input coefficients $c_1[k]$.

B. Practical Considerations

In most practical applications, the samples $y[k]$ of the output signal $y(t)$ are the desired end result. These can be calculated efficiently by post-filtering with $B_{\vec{\alpha}_2}(z)$ (the sampled version of the basis functions). This operator can be combined with the previous one into a single filter whose transfer function is

$$R_2(z) = \frac{B_{\vec{\alpha}_2}(z)}{\Delta_{\vec{\alpha}}(z)} = \frac{\sum_{k=0}^{N+N_1}\beta_{(\vec{\alpha}_1:\vec{\alpha})}(k)z^{-k}}{\prod_{n=1}^{N}(1-e^{\alpha_n}z^{-1})}.$$

Note that the corresponding digital filter is causal, rational of order N, and that it can be implemented recursively. It has poles that are in exact correspondence with those of its continuous-time counterpart. Thus, the proposed discretization procedure provides an efficient digital implementation that perfectly mimics the corresponding continuously defined system.

When the input signal is specified by its samples $x[k]$ rather than by its B-spline coefficients $c_1[k]$, we must also include the initial interpolation step. The block diagram describing the complete process is shown in Fig. 2. For the practitioner who is primarily interested in computing $y[k]$ from $x[k]$, these steps can all be combined into one global digital filter whose transfer function is

$$R_{12}(z) = \frac{R_2(z)}{B_{\vec{\alpha}_1}(z)} = \frac{\sum_{k=0}^{N+N_1}\beta_{(\vec{\alpha}_1:\vec{\alpha})}(k)z^{-k}}{\left(\sum_{k=0}^{N_1}\beta_{\vec{\alpha}_1}(k)z^{-k}\right)\prod_{n=1}^{N}(1-e^{\alpha_n}z^{-1})}.$$

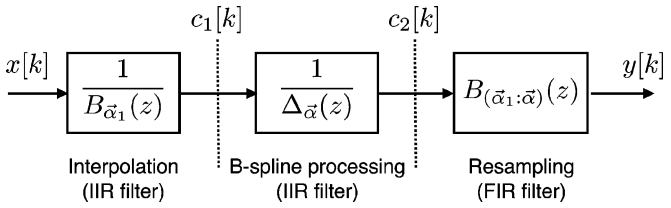

Fig. 2. Implementation of an analog filter in the B-spline domain.

It is interesting to note that for $N_1 = 0$ (the case of an ideally sampled input), the proposed technique is computationally equivalent to the impulse-invariance method, which produces a recursive digital filter whose impulse response is $\rho_{\vec{\alpha}}(k)$. However, it is important to emphasize that the interpretation of the process is quite different: The impulse-invariance method considers that the output signal is discrete (or eventually, bandlimited), whereas in our case, it is described by a continuous-time model (E-spline).

At any rate, the case $N_1 = 0$ is quite extreme because the bandwidth of the input signal is infinite, which can lead to aliasing artifacts when the output $y(t)$ is converted back to discrete form. From our point of view, it makes better sense to represent the input signal by a polynomial spline of order $N_1 \geq 1$; typically, $N_1 = 1$ (piecewise constant) or $N_1 = 2$ (piecewise linear). By increasing the order N_1, we can construct an equivalent digital filter that is arbitrarily close to the response of the continuous one over the entire Nyquist band. This is because 1) the proposed discretization procedure is exact for the underlying signal representation, and 2) the input signal will tend to be increasingly more bandlimited as N_1 increases [23].

C. Design Example

One of the preferred strategies for designing recursive filters is to start with an analog filter prototype and to apply some A to D mapping technique, such as the impulse-invariance method or the bilinear transform, to transpose it into the discrete domain [20]. The reason for this is that there are powerful analog design techniques that yield closed-form solutions (e.g., Butterworth and Chebyshev filters), which have no direct counterpart in the discrete domain. Interestingly, low-order designs tend to be the most challenging for the standard conversion techniques because they are more prone to aliasing artifacts. The technique that we are proposing here does not have this problem—the implementation is exact provided that one thinks in terms of splines—and may therefore be an interesting alternative.

To illustrate the procedure, we consider the discrete implementation of the first-order Butterworth filter $H(s) = -\alpha/(s-\alpha) = -\alpha H_\alpha(s)$ with $\alpha = -\log 2$. The corresponding localization filter is $\Delta_\alpha(z) = 1 - (1/2)z^{-1}$. The recursive filters $R_{12}(z)$ obtained for three input spline models of increasing order N_1 are

- ideal sampling model with $N_1 = 0$: $R_{12}(z) = 0.6931/(1 - 0.5z^{-1})$;
- piecewise-constant input with $N_1 = 1$ and $\vec{\alpha}_1 = (0)$: $R_{12}(z) = 0.5z^{-1}/(1 - 0.5z^{-1})$;
- piecewise-linear input with $N_1 = 2$ and $\vec{\alpha}_1 = (0, 0)$: $R_{12}(z) = 0.2786 + 0.2213z^{-1}/(1 - 0.5z^{-1})$.

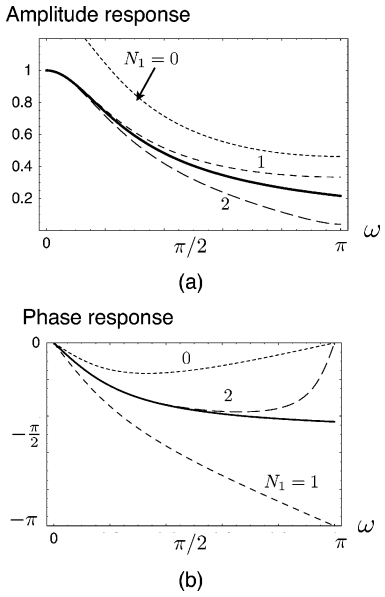

Fig. 3. Comparison of the frequency responses (amplitude and phase) for three filter designs using input models of increasing order. The response of the analog prototype (first-order Butterworth filter) is represented with a thick line.

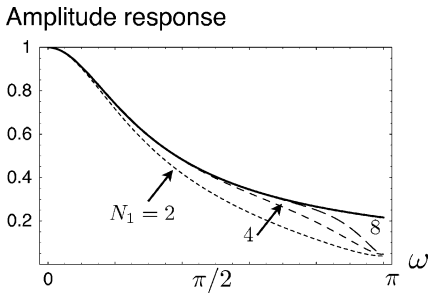

Fig. 4. Approximation of the frequency response of a first-order Butterworth filter for input spline models of increasing orders $N_1 = 2, 4$, and 8.

Their amplitude and phase responses are shown in Fig. 3 and compared to the characteristics of the analog filter $H(j\omega)$. As expected, the least favorable response is obtained for $N_1 = 0$, which also corresponds to the standard impulse invariance method. This filter does not even reproduce the unit gain at the origin, which is not very satisfactory for a lowpass design. The filters based on higher order splines do not have this defect because the underlying input models (polynomial splines) can reproduce the constant (polynomial of degree 0). The amplitude characteristic of the second filter is quite good, but its phase response is significantly different from the reference one. The third filter has by far the best phase response, as well as the amplitude response that is the closest to the analog one at low frequencies. However, it tends to attenuate higher frequencies more strongly than the prototype (which is not necessarily bad for a lowpass filter). Fig. 4 illustrates the property that we can match the frequency response of the analog filter as closely as we wish by increasing the order N_1 of the input spline model. However, there is a catch: The filters associated with these higher order models (here, cubic with $N_1 = 4$ and septimic splines with $N_1 = 8$) are no longer causal; yet, they can still be implement recursively using the algorithm described in [24].

Unlike the impulse-invariance method, the proposed procedure is also applicable for the design of bandpass or even highpass filters. In such cases, it is judicious to replace the polynomial spline input model by a modulated one with poles matching the resonance frequencies of the analog filter. This will have two beneficial effects: 1) It will ensure a good match of the discrete and analog frequency responses around those frequencies, and 2) it will help reducing aliasing artifacts because the bandwidth of the input signal is adapted to the filter characteristics.

V. Hybrid Signal Processing

The proposed framework is ideally suited for designing hybrid systems that combine analog and discrete signal processing components. In this section, we describe three such systems that rely on digital filtering techniques to correct for distortions incurred by nonideal A-to-D and D-to-A conversion. Their design is based on the generalized sampling theory for nonideal acquisition devices proposed in [25], which is briefly reviewed in Section V-A. All three systems reconstruct an analog signal $y(t)$ that is undistinguishable from the original input, at least, as far as the measurement system (nonideal sampling device) is concerned.

A. Review of Generalized Sampling

The generalized sampling theory presented in [25] provides a method for reconstructing an unknown input signal $x(t) \in L_2$ from a series of measurements $c_1[k] = \langle x(t), \varphi_1(t-k)\rangle$ in a given "shift-invariant" function space $V_2 = \text{span}\{\varphi_2(t-k)\}_{k\in\mathbb{Z}}$. Among all possible reconstructions of the form $y(t) = \sum_{k\in\mathbb{Z}} c_2[k]\varphi_2(t-k)$, there is only one that is *consistent* with $x(t)$ in the sense that it has exactly the same measurements: $\forall k \in \mathbb{Z}$, $\langle x(t), \varphi_1(t-k)\rangle = \langle y(t), \varphi_1(t-k)\rangle$. Theorem 1 in [25] states that the coefficients of this optimal solution are given by $c_2[k] = (q * c_1)[k]$, where q is the digital filter whose transfer function is

$$Q(z) = \frac{1}{\sum\limits_{k\in\mathbb{Z}} \langle \varphi_1(t-k), \varphi_2(t)\rangle z^{-k}}. \tag{23}$$

This solution corresponds to the oblique projection of $x(t)$ onto V_2 perpendicular to $V_1 = \text{span}\{\varphi_1(t-k)\}_{k\in\mathbb{Z}}$ (see also [26]). The sampling theory guarantees that the filter is stable and well-defined, provided that the cosine of the angle between the two spaces V_1 and V_2 is nonzero. It also provides an optimal error bound that compares this solution to the optimal least-squares approximation that is typically not realizable.

B. Consistent Sampling System

We consider the application of this theory to the case of a realistic A-to-D conversion system that uses an analog lowpass filter prior to sampling to reduce aliasing artifacts. We seek to reconstruct an output signal $y(t)$ that is a E-spline with parameter $\vec{\alpha}_2$ that corresponds to the choice $\varphi_2(t) = \beta_{\vec{\alpha}_2}(t)$ in our generalized sampling formulation. We also assume that the analog prefilter is given to us and that it has a rational transfer function $H_1(s)$ of the form (6) with poles $\{\alpha_{1,n}\}_{n=1,\ldots,N_1}$ and zeros $\{\gamma_{1,m}\}_{m=1,\ldots,M_1}$. This model is rich enough to specify any physical system described by ordinary differential equations

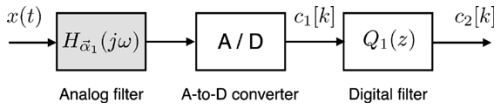

Fig. 5. Consistent sampling system: the input signal $x(t)$ is prefiltered in the continuous-time domain prior to sampling (A-to-D conversion). The measured samples are then corrected by digital filtering so that the underlying signal model $y(t) = \sum_{k\in\mathbb{Z}} c_2[k]\beta_{\vec{\alpha}_2}(t-k)$ is a consistent spline approximation of the input.

(e.g., electric circuit). The sampling is performed by a standard sample-and-hold, A-to-D converter, which yields the discrete samples $c_1[k]$ (measurements). What we are proposing here is to add a digital post-filtering step to compensate for the fact that the analog prefilter $H_1(s)$ is nonideal and that it introduces amplitude and phase distortions. The corresponding block diagram is represented in Fig. 5. As in Section IV, we use the fact that $\rho_{\vec{\alpha}_1}(t) = \varphi_1(-t)$ (the impulse response of $H_1(s)$) is an E-spline with parameter $\vec{\alpha}_1$ that satisfies the Green-function reproduction formula (1). To determine the optimal correction filter $Q_1(z)$, we evaluate the convolution product

$$(\rho_{\vec{\alpha}_1} * \varphi_2)(t) = \left(\sum_{k\in\mathbb{Z}} p_{\vec{\alpha}_1}[k]\, \beta_{\vec{\alpha}_1}(t-k)\right) * \beta_{\vec{\alpha}_2}(t) \tag{24}$$

$$= \sum_{k\in\mathbb{Z}} p_{\vec{\alpha}_1}[k]\, \beta_{(\vec{\alpha}_1:\vec{\alpha}_2)}(t-k) \tag{25}$$

which is a spline of increased order $N_1 + N_2$. By plugging this result into (23) and recalling that $P_{\vec{\alpha}_1}(z) = 1/\Delta_{\vec{\alpha}_1}(z)$, we obtain the transfer function of the optimal correction filter for the system in Fig. 5:

$$Q_1(z) = \frac{\Delta_{\vec{\alpha}_1}(z)}{\sum\limits_{k=0}^{N_1+N_2} \beta_{(\vec{\alpha}_1:\vec{\alpha}_2)}(k) z^{-k}} \tag{26}$$

where $\Delta_{\vec{\alpha}_1}(z) = \prod_{n=1}^{N_1}(1 - e^{\alpha_{1,n}} z^{-1})$. Based on the interpretation given in Section II-B, we see that this latter FIR filter is a discrete approximation of the differential operator that compensates the allpole component (denominator) of $H_1(s)$. The B-spline part in the numerator of (26) refines this correction to have a consistent solution while also taking into account the differential part (numerator) of $H_1(s)$. In fact, it corresponds to the interpolation filter for the augmented-order spline space $V_{(\vec{\alpha}_1:\vec{\alpha}_2)}$. In most cases, the corresponding infinte impulse response (IIR) correction filter will be stable—but not necessarily causal—meaning that it can be implemented recursively using the procedure described in [18, Sec. IV.A]. For special situations where the interpolation problem is ill-posed, it is, in principle, possible to introduce a noninteger shift in the response to stabilize the filter, as discussed in [18].

C. Digitally Compensated D-to-A Conversion

We now consider the D-to-A conversion problem that is the converse of the preceding one. We are given a discrete input signal $x[k]$, and we want to design a D-to-A conversion system that generates a continuously defined output signal $y(t)$ that interpolates these samples exactly, i.e., $\forall k \in \mathbb{Z}$, $y(t)|_{t=k} = x[k]$. Our system utilizes standard electronic components: 1) an off-the-shelf D-to-A converter that produces a piecewise-constant output (first-order polynomial spline interpolator) and

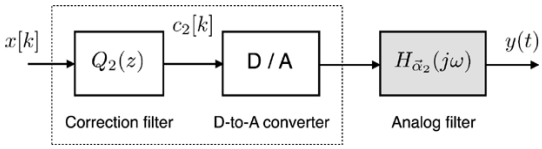

Fig. 6. Digitally compensated D-to-A convertor: The signal samples are digitally prefiltered prior to D-to-A conversion to ensure that the output signal $y(t)$ is a correct interpolation of the input.

2) an analog postfilter that smoothes out the response of the convertor. There are two well-documented problems associated with such a circuit: First, the D-to-A converter, which uses $\beta_{(0)}(t)$ as basis function, will distort the in-band portion of the Fourier spectrum of the input signal by multiplying it with a sinc function—the so-called "droop" effect. Second, the analog output filter, which is intended to suppress the out-of-band frequency components, will necessarily introduce distortions; in particular, some phase distortion because its impulse response is causal. Here, we are proposing to include a digital prefilter q_2 in the chain to compensate for these effects. The corresponding system is shown in Fig. 6.

As in the previous case, we assume that the analog filter has a rational transfer function $H_2(s)$ of the form (6) with poles $\{\alpha_{2,n}\}_{n=1,...,N_2}$ and zeros $\{\gamma_{2,m}\}_{m=1,...,M_2}$. Its impulse response, which is denoted by $\rho_{\vec{\alpha}_2}(t)$, is an E-spline with parameter $\vec{\alpha}_2$, which can be represented by its B-spline expansion (1). We now reformulate the problem so that we can apply the sampling theory in Section V-A to derive the digital correction filter. To this end, we note that the required interpolation condition can be rephrased as a consistency requirement with $\varphi_1(t) = \delta(t)$. The digital filtering of the input signal yields the coefficients $c_2[k] = (q_2 * x)[k]$, which are fed into the D-to-A convertor. After analog filtering, the resulting output signal is given by $y(t) = \sum_{k\in\mathbb{Z}} c_2[k]\varphi_2(t-k)$ with $\varphi_2(t) = \beta_{(0)}(t) * \rho_{\vec{\alpha}_2}(t)$. Next, we evaluate the cross-correlation function $\langle \varphi_1(\cdot - \tau), \varphi_2(\cdot)\rangle = \sum_{n\in\mathbb{Z}} p_{\vec{\alpha}_2}[n]\beta_{(0:\vec{\alpha}_2)}(\tau - n)$ using our B-spline calculus. By plugging this result into (23) and recalling that $P_{\vec{\alpha}_2}(z) = 1/\Delta_{\vec{\alpha}_2}(z)$, we obtain the transfer function of the optimal correction filter for the system in Fig. 6:

$$Q_2(z) = \frac{\Delta_{\vec{\alpha}_2}(z)}{\sum_{k=0}^{N_2+1} \beta_{(0:\vec{\alpha}_2)}(k) z^{-k}}. \tag{27}$$

As example of design, we consider the case of a second-order, allpole smoothing filter with $\vec{\alpha}_2 = (-1, -2)$. The corresponding digital filter that is obtained from (27) is

$$Q_2(z) = z \cdot \frac{1 - 0.5032z^{-1} + 0.049\,79z^{-2}}{0.1998 + 0.073\,50z^{-1}}.$$

It is composed of a stable, causal filter (with a pole at $z_0 = -0.367$) that can be implemented recursively in real time. The presence of the factor z in the transfer function is not too surprising since the system needs to correct for the phase distorsion of the analog filter. Practically, this means that the output will be delayed by one sample with respect to the input. Fig. 7 illustrates the type of output signal that is provided by this system and compares the solution to a simple sample-and-hold reconstruction. Despite the fact that the analog filtering is relatively

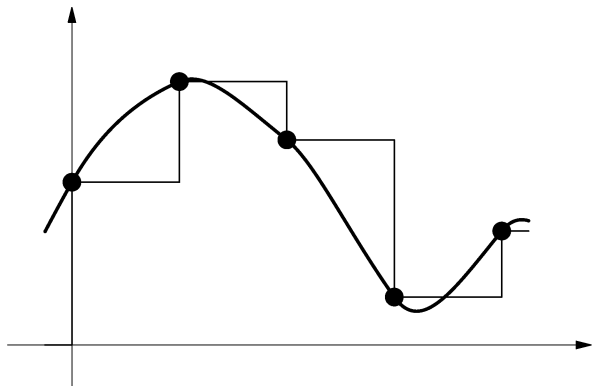

Fig. 7. Comparison between the outputs of two D-to-A convertors. (a) Piecewise-constant reconstruction. (b) Second-order digitally compensated system with $\vec{\alpha}_2 = (-1, -2)$.

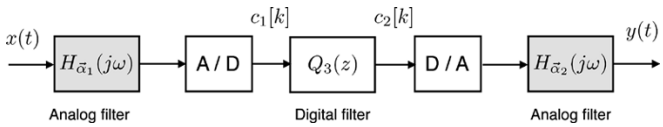

Fig. 8. High-fidelity reproduction. This system produces a consistent reconstruction of an analog input signal from a series of equally spaced measurements (samples). It includes a digital correction filter that compensates the distortions introduced by the two analog filters that are used in conjunction with the A-to-D and D-to-A converters.

mild, the output signal is smooth (in fact, $y(t)$ is twice-differentiable) and does not present visible reconstruction artifacts. The generated output signal is such that it interpolates the input samples perfectly.

We believe that the present solution is an interesting alternative to the more complex quadratic spline interpolation circuit that has been proposed by Kamada *et al.* [27], [28]. The advantage of the present design is that it requires no active components such as integrators, which tend to drift.

D. High-Fidelity Reproduction System

Finally, we consider a beginning-to-end system where the input and output signals are analog, but the intermediate representation (storage or transmission) is digital. The standard approach for this type of problem is modular. For instance, one may simply combine the solutions for A-to-D and D-to-A conversion that have just been proposed. We believe that we can do better by looking at the problem in its entirety and applying the same methodology as before to specify a solution that is globally optimal.

The corresponding hybrid system is summarized in Fig. 8; it qualifies as a high-fidelity reproduction system because its output is undistinguishable from its input on the basis of the measurements that are performed. For instance, if this was a hypothetical sound recording/reproduction system with an input microphone and an output speaker, the system specification would ensure that one would record exactly the same sound again if one would replace the initial source by the acoustic output of the system. Because the solution of the generalized sampling problem is unique, there is only one digital filter q_3 that can ensure this property for arbitrary input signals, with

no restriction whatsoever (in particular, the input need not be bandlimited).

The relevant analysis and synthesis functions are now $\varphi_1(t) = \rho_{\vec{\alpha}_1}(-t)$ and $\varphi_2(t) = \left(\beta_{(0)} * \rho_{\vec{\alpha}_2}\right)(t)$, which is a mix between the formulations in Sections V-B and C. To determine the optimal solution, we compute the cross-correlation function $\langle \varphi_1(\cdot - \tau), \varphi_2(\cdot) \rangle$, which is done by using the same technique as before. This ultimately yields the globally optimal correction filter

$$Q_3(z) = \frac{\Delta_{\vec{\alpha}_1}(z)\Delta_{\vec{\alpha}_2}(z)}{\sum_{k=0}^{N_1+N_2+1} \beta_{(\vec{\alpha}_1:0:\vec{\alpha}_2)}(k) z^{-k}}$$

which is generally IIR and can be implemented recursively.

VI. Conclusion

In this paper, we introduced an extended family of cardinal E-splines, where each type is associated with a continuous-time differential system. Practically, this means that a spline family is specified by a list of poles and zeros in essentially the same way as one describes an analog filter. Schoenberg's polynomial splines, for instance, correspond to a system whose poles are all placed at the origin.

Cardinal E-splines have several important properties that make them particularly attractive for signal processing.

- *B-spline representation:* They can be expressed very efficiently in terms of compactly supported basis functions (B-spline expansion).
- *Continuous-time signal processing:* The family is closed with respect to the primary continuous-time signal processing operations: convolution, differential operators (including analog filters with rational transfer function), and modulation. These can be implemented directly by applying the discrete counterparts of these operations in the B-spline domain.
- *Ease of manipulation:* E-splines are as simple to manipulate as polynomial splines. In particular, spline fitting and approximation procedures can be implemented efficiently via recursive digital filtering.
- *Generality:* Our extended E-splines family contains all known brands of cardinal splines (polynomial, trigonometric, hyperbolic, and exponential splines), as well as other families of functions such as the OMOMS that had not been catalogged as splines thus far. The bandlimited model is also included as a limiting case since it can be assimilated to a spline of infinite order [23].

The proposed formalism has an interesting conceptual role in that it really brings together the continuous and discrete aspects of signal processing. In particular, it explains why there is such a strong resemblance between the basic continuous-time and discrete-time results of linear systems' theory. There are also practical benefits because the proposed spline calculus simplifies the mathematical analysis of hydrid signal processing systems while, at the same time, suggesting some new solutions. We believe that these methods may also be useful for the digital simulation of analog circuits and that they are well-suited for control applications that are increasingly relying on digital controllers.

We have presented some examples of hybrid signal processing to illustrate the ease of use of our spline-based formalism. The designs were kept simple on purpose to demonstrate the type of signal processing tasks that could benefit from our techniques. To make these systems really practical, one would need to optimize the analog filter parameters and consider higher order models. These applications also raise a number of theoretical issues that call for further investigations. What is the best analog reconstruction filter for a hybrid system? How can one take into account, and eventually reduce, the effect of measurement noise? Are there high-order configurations of poles and zeros that lead to compensation or interpolation filters that are causal, which would be advantageous for online processing? The answer to the last question, which is likely to be positive, is practically quite relevant and could represent a new interesting challenge for filter designers.

Appendix
Software for the Computation of B-Splines

To obtain the analytical expression of the generalized exponential B-splines and other related quantities, we recommend using a mathematical software package for symbolic manipulations. We have made an implementation available for Mathematica at http://bigwww.epfl.ch/demo/Esplines/. The spline type in each routine is specified by two list variables: poles, and zeros (which is optional). For example, the OMOMS in Section III-C corresponds to the parameters `poles` $= \{0, 0, 0, 0\}$ and `zeros` $= \{$`-I Sqrt[42], I Sqrt[42]`$\}$.

The available functions follow:

- BsplineE[`t`, poles, zeros] evaluates the generalized B-spline from (9);
- B[`z`, poles, zeros] returns the discrete B-spline filter $B(z) = \sum_{k=0}^{N} \beta_{\vec{\alpha}}(k) z^{-k}$;
- A[`z`, poles, zeros] returns the z-transform of the Gram sequence (14);
- Localization[`z`, poles] returns the z-transform of the localization operator (4);
- GreenE[`t`, poles, zeros] evaluates or returns the symbolic form (8) of the Green function $\rho_{\vec{\alpha}}(t)$, which is obtained by inverse Laplace transformation of (6).

Acknowledgment

The author is most grateful to Prof. F. Pellandini, who introduced him to the pleasures of teaching the "Signals and Systems" course at the EPFL and who got him thinking further. This had a profound impact on the present research.

References

[1] D. Slepian, "On bandwidth," *Proc. IEEE*, vol. 64, pp. 292–300, 1976.
[2] I. Daubechies, "Orthogonal bases of compactly supported wavelets," *Commun. Pure Appl. Math.*, vol. 41, pp. 909–996, 1988.
[3] S. Mallat, *A Wavelet Tour of Signal Processing*. San Diego, CA: Academic, 1998.
[4] G. Strang and T. Nguyen, *Wavelets and Filter Banks*. Wellesley, MA: Wellesley-Cambridge, 1996.

[5] S. G. Mallat, "A theory of multiresolution signal decomposition: The wavelet representation," *IEEE Trans. Pattern Anal. Machine Intell.*, vol. 11, no. 7, pp. 674–693, Jul. 1989.
[6] P. Flandrin, "Wavelet analysis and synthesis of fractional Brownian motion," *IEEE Trans. Inf. Theory*, vol. 38, no. 2, pp. 910–917, Mar. 1992.
[7] S. Mallat and W. L. Hwang, "Singularity detection and processing with wavelets," *IEEE Trans. Inf. Theory*, vol. 38, no. 2, pp. 617–643, Mar. 1992.
[8] P. Thévenaz, T. Blu, and M. Unser, "Interpolation revisited," *IEEE Trans. Med. Imag.*, vol. 19, no. 7, pp. 739–758, Jul. 2000.
[9] E. Meijering, "A chronology of interpolation: From ancient astronomy to modern signal and image processing," *Proc. IEEE*, vol. 90, no. 3, pp. 319–342, Mar. 2002.
[10] T. I. Laakso, V. Välimäki, M. Karjalainen, and U. K. Laine, "Splitting the unit delay: Tools for fractional delay filter design," *IEEE Signal Process. Mag.*, vol. 13, no. 1, pp. 514–543, Jan. 1996.
[11] S. C. Pei and C. C. Tseng, "An efficient design of a variable fractional delay filter using a first-order differentiator," *IEEE Signal Process. Lett.*, vol. 10, pp. 307–310, Oct. 2003.
[12] B. Kumar, S. C. D. Roy, and H. Shah, "On the design of FIR digital differentiators which are maximally linear at the frequency π/p, $p \in \{\text{positive integers}\}$," *IEEE Trans. Signal Process.*, vol. 40, no. 9, pp. 2334–2338, Sep. 1992.
[13] S. Sunder and R. P. Ramachandran, "Least-squares design of higher order nonrecursive differentiators," *IEEE Trans. Signal Process.*, vol. 42, no. 4, pp. 956–961, Apr. 1994.
[14] S. C. Pei and P. H. Wang, "Closed-form design of maximally flat FIR Hilbert transformers, differentiators, and fractional delayers by power series expansion," *IEEE Trans. Circuits Syst. I: Funda. Theory Appl.*, vol. 48, no. 4, pp. 389–398, Apr. 2001.
[15] I. W. Selesnick, "Maximally flat low-pass digital differentiators," *IEEE Trans. Circuits Syst. II: Analog Digit. Signal Process.*, vol. 49, no. 3, pp. 219–223, Mar. 2002.
[16] R. E. Crochiere and L. R. Rabiner, "Interpolation and decimation of digital signals," *Proc. IEEE*, vol. 69, pp. 300–331, 1981.
[17] A. I. Russell and P. E. Beckmann, "Efficient arbitrary sampling rate conversion with recursive calculation of coefficients," *IEEE Trans. Signal Processing*, vol. 50, no. 4, pp. 854–865, Apr. 2002.
[18] M. Unser and T. Blu, "Cardinal exponential splines: Part I—Theory and filtering algorithms," *IEEE Trans. Signal Process.*, vol. 53, no. 4, pp. 1425–1438, Apr. 2005.
[19] A. V. Oppenheim and A. S. Willsky, *Signal and Systems*. Upper Saddle River, NJ: Prentice-Hall, 1996.
[20] B. P. Lathy, *Signal Processing and Linear Systems*. Carmichael, CA: Berkeley-Cambridge, 1998.
[21] L. L. Schumaker, *Spline Functions: Basic Theory*. New York: Wiley, 1981.
[22] T. Blu, P. Thévenaz, and M. Unser, "MOMS: Maximal-order interpolation of minimal support," *IEEE Trans. Image Process.*, vol. 10, no. 7, pp. 1069–1080, Jul. 2001.
[23] A. Aldroubi, M. Unser, and M. Eden, "Cardinal spline filters: Stability and convergence to the ideal sinc interpolator," *Signal Process.*, vol. 28, no. 2, pp. 127–138, 1992.
[24] M. Unser, A. Aldroubi, and M. Eden, "B-spline signal processing: Part II—Efficient design and applications," *IEEE Trans. Signal Process.*, vol. 41, no. 2, pp. 834–848, Feb. 1993.
[25] M. Unser and A. Aldroubi, "A general sampling theory for nonideal acquisition devices," *IEEE Trans. Signal Process.*, vol. 42, no. 11, pp. 2915–2925, Nov. 1994.
[26] M. Unser, "Sampling—50 years after Shannon," *Proc. IEEE*, vol. 88, no. 4, pp. 569–587, Apr. 2000.
[27] M. Kamada, K. Toraichi, and R. E. Kalman, "A smooth signal generator based on quadratic B-spline functions," *IEEE Trans. Signal Process.*, vol. 43, no. 5, pp. 1252–1255, May 1995.
[28] ——, "Quadratic spline interpolator," *Int. J. Syst. Sci.*, vol. 27, no. 10, pp. 977–983, 1996.

Michael Unser (M'89–SM'94–F'99) received the M.S. (summa cum laude) and Ph.D. degrees in electrical engineering in 1981 and 1984, respectively, from the Swiss Federal Institute of Technology (EPFL), Lausanne, Switzerland.

From 1985 to 1997, he was with the Biomedical Engineering and Instrumentation Program, National Institutes of Health, Bethesda, MD. He is now Professor and Head of the Biomedical Imaging Group at EPFL. His main research area is biomedical image processing. He has a strong interest in sampling theories, multiresolution algorithms, wavelets, and the use of splines for image processing. He is the author of 100 published journal papers in these areas.

Dr. Unser is Associate Editor-in-Chief for the IEEE TRANSACTIONS ON MEDICAL IMAGING. He is on the editorial boards of several other journals, including IEEE SIGNAL PROCESSING MAGAZINE, *Signal Processing*, IEEE TRANSACTIONS ON IMAGE PROCESSING (from 1992 to 1995), and IEEE SIGNAL PROCESSING LETTERS (from 1994 to 1998). He serves as regular chair for the SPIE Conference on Wavelets, which has been held annually since 1993. He was general co-chair of the first IEEE International Symposium on Biomedical Imaging, Washington, DC, 2002. He presently chairs the newly formed technical committee on Bio Imaging and Signal Processing (BISP) of the IEEE Signal Processing Society, from which he also received the 1995 and 2003 Best Paper Awards and the 2000 Magazine Award.